Journal of Molecular Catalysis A: Chemical 301 (2009) 67–78

Contents lists available at ScienceDirect

Journal of Molecular Catalysis A: Chemical

journal homepage: www.elsevier.com/locate/molcata

Solvent free synthesis of 7-isopropyl-1,1-dimethyltetralin by the rearrangement of longifolene using nano-crystalline sulfated zirconia catalyst

Beena Tyagi*, Manish K. Mishra[1], Raksh V. Jasra**

Discipline of Inorganic Materials and Catalysis, Central Salt and Marine Chemicals Research Institute (CSMCRI), Council of Scientific and Industrial Research (CSIR), GB Marg, Bhavnagar 364002, Gujarat, India

ARTICLE INFO

Article history:
Received 8 February 2008
Received in revised form 6 November 2008
Accepted 10 November 2008
Available online 19 November 2008

Keywords:
Nano-crystalline sulfated zirconia
Longifolene rearrangement
Longifolene isomerization
Isolongifolene
7-Isopropyl-1,1-dimethyltetralin

ABSTRACT

Nano-crystalline sulfated zirconia solid acid catalyst, synthesized by a one-step sol–gel method, was studied for the rearrangement of longifolene to isolongifolene and 7-isopropyl-1,1-dimethyltetralin under solvent free conditions. Kinetic and ^{1}H NMR spectroscopic studies confirmed the formation of 7-isopropyl-1,1-dimethyltetralin through further rearrangement of isolongifolene in the presence of a higher number of acidic sites. The selectivity for the rearranged products namely isolongifolene and 7-isopropyl-1,1-dimethyltetralin was observed to be strongly influenced by the acidity of the catalysts in terms of Brönsted (B) and Lewis (L) acid sites ratio. The catalyst having a higher B/L ratio (5.6) showed higher selectivity (56%) for 7-isopropyl-1,1-dimethyltetralin. The selectivity for the products could also be controlled by longifolene to catalyst weight ratio; for example, ~100% isolongifolene could be obtained using less amount of the catalyst, whereas for 7-isopropyl-1,1-dimethyltetralin higher amount of catalyst was required. Thermally regenerated catalyst showed decreased selectivity for 7-isopropyl-1,1-dimethyltetralin due to a decrease in the B/L ratio, which in turns influenced by loss of sulfur during the reaction.

1. Introduction

The sulfated zirconia is a potential catalyst for the isomerization of *n*-alkanes at ambient temperature and has been extensively studied for the isomerization of *n*-butane [1–4], higher *n*-alkanes [5], cycloalkanes [6] and alkenes [7]. It has also been used for other various acid catalyzed reactions such as alkylation, acylation, esterification, etherification, nitration, oligomerization. [8,9]. However, there are few studies reported for the synthesis of fine chemicals by the isomerization of terpenes using sulfated zirconia catalyst [10–12].

Longifolene, $C_{15}H_{24}$ (decahydro-4,8,8-trimethyl-9-methylene-1-4-methanoazulene), a tricyclic sesqui-terpene hydrocarbon, is a commercially important chemical and is used in perfumery industry owing to its woody odor [13]. It occurs in Indian turpentine oil (5–10%), which is produced commercially from the Himalayan pine, *Pinus Longifolia*. Longifolene may undergo different acid catalyzed rearrangements depending on the reaction conditions, reagents and particularly on the acidity of the catalyst. In the presence of strong protic acids such as H_2SO_4 or Lewis acids such as BF_3–Et_2O, longifolene (I) isomerizes selectively to isolongifolene (II) (Scheme 1) [14–16], which is also used in perfumery industries due to its woody amber odor [17]. However, under severe reaction conditions, for example, by refluxing (5 h) the isolongifolene with silica gel–H_3PO_4/Amberlyst-15 or continued reaction of longifolene with BF_3–Et_2O (14 h at room temperature), formation of tetralin (III) and octalin (IV) aromatic hydrocarbons was observed (Scheme 1) [18]. Therefore, the severe reaction conditions seem to result in further rearrangement of isolongifolene to tetralin derivatives.

Tetralin, i.e., tetrahydronaphthalene, itself is used as a high-boiling solvent, whereas tetralin derivatives have varied applications. For example, substituted tetralin derivatives, known as Tonalide®, Fixolide® and Versalide® that belong to the group of polycyclic musk fragrances, are used in cosmetics and laundry detergents and are of industrial importance. Tetralin derivatives have important pharmaceutical applications such as Ghrelin (an acylated peptide for stimulating the release of growth hormone) receptor modulators, anti-arrhythmic agents in cardiovascular problems, anti-glaucoma agents and local anesthetic agents. Resin mixtures having 1-oxa-3-aza tetralin group are used as fire retardant curable.

In our previous study [19] on the isomerization of longifolene using nano-crystalline sulfated zirconia catalyst, we found >90% conversion and ~100% selectivity for isolongifolene under solvent free conditions at 180 °C in 15 min. We did not observe the for-

* Corresponding author. Tel.: +91 278 2471793; fax: +91 278 2567562.
** Corresponding author. Present address: R & D Centre, Reliance Technology Group, Reliance Industries Limited, Vadodara Manufacturing Division, Vadodara 391346, Gujarat, India. Tel.: +91 265 6603935/278 2471793; fax: +91 265 6693934/278 2567562.
E-mail addresses: btyagi@csmcri.org (B. Tyagi), rakshvir.jasra@ril.com (R.V. Jasra).
[1] Tel.: +91 278 2471793; fax: +91 278 2567562.

1381-1169/$ – see front matter © 2008 Elsevier B.V. All rights reserved.
doi:10.1016/j.molcata.2008.11.011

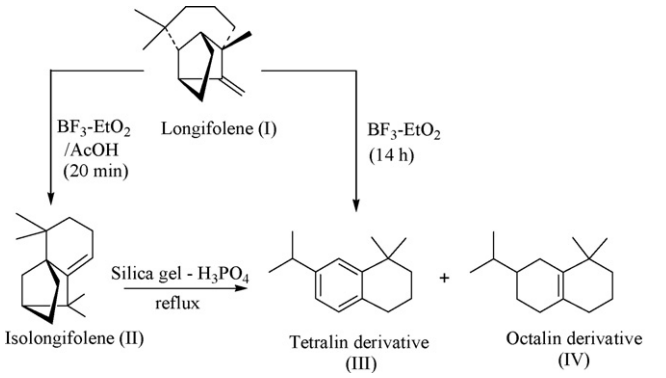

Scheme 1. Rearrangement of Longifolene using homogenous and acidic silica gel catalysts.

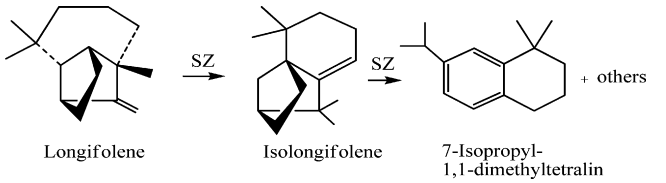

Scheme 2. Rearrangement of Longifolene using nano-crystalline sulfated zirconia catalyst.

mation of any other rearranged product or aromatic hydrocarbons even when the reaction was carried out for longer time (6 h). In the present work, we report the catalytic activity of the nano-crystalline sulfated zirconia catalyst, synthesized by a one-step sol–gel method, for rearrangement of longifolene to 7-isopropyl-1,1-dimethyltetralin under solvent free conditions (Scheme 2). Based on kinetic and ^{1}H NMR spectroscopic studies the reaction pathways for the formation of 7-isopropyl-1,1-dimethyltetralin from longifolene via isolongifolene are discussed. The novelty of the present study lies in the observation that the sulfated zirconia catalyst is useful for obtaining different rearranged products under similar reaction conditions only by varying the amount of the catalyst showing thereby that the product selectivity can be controlled by the catalyst concentration. To the best of our knowledge, it is the first report of the synthesis of 7-isopropyl-1,1-dimethyltetralin by the rearrangement of longifolene using solid acid catalyst.

2. Experimental

2.1. Materials

Zirconium propoxide (70 wt% solution in 1-propanol) was procured from Sigma–Aldrich, USA and was used after dilution with 1-propanol (30 wt%); 1-propanol, aqueous ammonia (25%) and concentrated sulfuric acid were from s.d. Fine chemicals, India. Longifolene was procured from Dhruv Aroma Chemicals, Vadodara, India and was used after distillation (~79%).

2.2. Catalyst synthesis

The sulfated zirconia catalyst was synthesized using a one-step sol–gel technique [20]. In a typical experiment, concentrated sulfuric acid was added to zirconium propoxide precursor and distilled water was added dropwise under continuous stirring, just sufficient to form a gel. The resulting gel was dried at 110 °C for 12 h and calcined at different temperatures of 600, 700 and 800 °C for 2 h in static air. The catalysts thus prepared were designated as SZ-600, SZ-700 and SZ-800, respectively.

2.3. Catalyst characterization

2.3.1. Powder X-ray diffraction (PXRD)

The nature of crystalline phase formed and the crystallinity of sulfated zirconia samples after calcination at different temperatures were determined by a X-ray powder diffractometer (Philips X'pert) by using Cu Kα radiation (λ = 1.5405 Å). The samples were scanned in the 2θ range of 0–80° at a scanning rate of 0.04° s^{-1}. The crystallite size of the tetragonal phase was determined from the characteristic peak (2θ = 30.18 for the (1 1 1) reflection) by using Scherrer formula [21] with a shape factor (K) of 0.9 as shown below:

$$\text{crystallite size} = \frac{K\lambda}{W\cos\theta}$$

where $W = W\text{b} - W\text{s}$; Wb is the broadened profile width of experimental sample and Ws is the standard profile width of reference silicon sample.

2.3.2. FT-IR spectroscopy

The nature of bonding of sulfate ions with zirconia surface after calcination at different temperatures was studied by a FT-IR spectrophotometer (Perkin-Elmer GX, USA). The spectra were recorded in the range of 400–4000 cm^{-1} with a resolution of 4 cm^{-1} as KBr pellets.

2.3.3. Sulfur analysis

The bulk sulfur (wt%) retained in sulfated zirconia samples after calcination at different temperatures was analyzed by a CHNS/O elemental analyzer (Perkin-Elmer, 2400, Sr.II, USA). The bulk sulfur was also measured by inductively coupled plasma-OES (Perkin Elmer Instrument, Optima 200 DV) by using two methods: (i) by dissolving the sample (100 mg) in 40% HF solution (15–20 drops) followed by addition of 5% boric acid solution and make up to 100 ml for analysis (ii) by stirring the sample (100 mg) in 0.1N NaOH solution (100 ml) for 5 min [22] followed by filtration and acidification of filtrate using concentrated HCl (2 ml) for analysis.

2.3.4. Surface area, pore volume and pore size distribution

Specific surface area, pore volume and pore size distribution of sulfated zirconia samples after calcination at different temperatures were determined from N_2 adsorption–desorption isotherms measured at 77 K (ASAP 2010, Micromeritics, USA). Surface area was calculated by using the BET equation; pore volume and pore size distribution were calculated by the BJH method [23]. Prior to adsorption measurement, the samples were activated by *in situ* heating at 120 °C under vacuum (1×10^{-3} mmHg) for 4 h to evacuate the physisorbed moisture.

2.4. Surface acidity measurement

2.4.1. Temperature programmed desorption (TPD) of NH_3

The total surface acidity of sulfated zirconia samples, calcined at different temperatures, was measured by a Micromeritics Pulse Chemisorb 2720 instrument by using temperature programmed desorption of NH_3. The sample (0.1 g) taken in a reactor and was *in situ* activated at 400 °C for 1 h in helium gas (He) flow. After bringing down the reactor temperature to 120 °C, a mixture of 5% NH_3 with He was passed for 10 min to allow the chemisorption of ammonia. The excess physisorbed ammonia was flushed out with pure He gas flow at 120 °C for 1 h. The sample was then heated at a rate of 10 °C min^{-1} up to 700 °C and volume of desorbed NH_3 was measured.

2.4.2. Brönsted acidity by cyclohexanol dehydration

The Brönsted acidity of the samples was determined by a vapor phase cyclohexanol dehydration reaction in a fixed bed reactor. The sample (0.5 g) was packed in a glass reactor bed and *in situ* activated at 450 °C for 2 h under air flow (15 ml min^{-1}). The cyclohexanol (5 ml) was delivered by a syringe pump injector (Cole Parmer, 74900 series) at a flow rate of 0.042 ml min^{-1} under N_2 flow (15 ml min^{-1}) after bringing down the catalyst bed temperature to 175 °C. The product samples were collected after 1 h and analyzed with a gas chromatograph (HP 6890, having HP50 capillary column (30 m), FID detector, programmed oven temperature from 50 to 200 °C under N_2 flow (0.5 ml min^{-1}). The conversion of cyclohexanol was calculated on the basis of its weight percent; the initial theoretical weight percent of cyclohexanol was divided by initial GC peak area percent to get a response factor. Final unreacted weight percent of cyclohexanol remaining in the reaction mixture was calculated by multiplying the response factor with the GC peak area percent for cyclohexanol obtained after the reaction. The conversion of cyclohexanol and selectivity were calculated as follows:

$$\text{conversion of cyclohexanol (wt\%)} = 100 \times \left[\frac{\text{initial wt\%} - \text{final wt\%}}{\text{initial wt\%}}\right]$$

$$\text{selectivity for cyclohexene (wt\%)} = 100 \times [\text{GC peak area \% of cyclohexene}] / \Sigma\ \text{GC peak area \% of all the products.}$$

2.4.3. Diffuse reflectance FT-IR (DRIFT) spectroscopy of pyridine adsorption

The Brönsted and Lewis acidity of the samples was ascertained by DRIFT spectroscopy after pyridine adsorption. The sample (0.2 g, pre-activated at 450 °C, 2 h) was exposed to dry pyridine vapors (25 ml) in a desiccator for 1 h under vacuum. Subsequently, the sample was evacuated at room temperature for 30 min to desorb physisorbed pyridine. DRIFT spectra were recorded on a FT-IR spectrophotometer (Perkin Elmer Spectrum GX) equipped with 'The Selector' DRIFT accessory (Graseby Specac, P/N 19900 series), initially at room temperature under dry N_2 flow (30 cm^3 min^{-1}) and then after heating to 150 °C. The sample was held at 150 °C for 15 min, thus allowing sufficient time for the desorption of pyridine before recording the spectra. Typically 30 scans were co-added for recording the spectra at a resolution of 4 cm^{-1} with a standard mid-IR DTGS detector and a germanium coated KBr beam splitter.

2.5. Theoretical calculations

The free energy and entropy for the stable structures of longifolene, isolongifolene and 7-isopropyl-1,1-dimethyltetralin at 25 °C were calculated by Materials Studio (Version 4.1, Accelrys Inc., San Diego, USA) by using DFT program DMol3.

2.6. Catalytic activity: rearrangement of longifolene

The catalytic rearrangement of longifolene was carried out in a liquid phase batch reactor. Typically, longifolene and the catalyst (pre-activated at 450 °C for 2 h, with longifolene to catalyst weight ratio of 10) were heated to optimized temperature of 180 °C [19] for 1 h under stirring in a 50 ml reaction tube of a reaction station (12 Place Heated Carousel Reaction Station, RR99030, Radleys Discovery Technologies, UK). Following this, the reaction mixture was filtered to separate the catalyst and was analyzed with a gas chromatograph (HP 6890 having specifications as described in Section 2.4.2). The conversion of longifolene and the selectivity for the rearranged products namely isolongifolene (II) and 7-isopropyl-1,1-dimethyltetralin (III) were calculated as follows:

$$\text{conversion of longifolene (wt\%)} = 100 \times \left[\frac{\text{initial wt\%} - \text{final wt\%}}{\text{initial wt\%}}\right]$$

$$\text{selectivity for (II) or (III)} = 100 \times [\text{GC peak area \% of (II) or (III)}] / \Sigma\ \text{GC peak area \% of all the products}$$

The product 7-isopropyl-1,1-dimethyltetralin was separated by column chromatography using silica gel (100–200 mesh) and petroleum ether and was identified by ^{1}H NMR spectroscopy (Bruker, Avance DPX 200 MHz) and GC–MS (Shimadzu GC MS-QP 2010), having a Petrocol capillary column (50 m × 0.2 mm), a programmed oven temperature from 40 to 250 °C, under He flow (1.2 cm^3 min^{-1}) and ion source temperature at 273 °C). The other rearranged products were identified by GC–MS analysis of the reaction mixture.

2.7. Catalyst regeneration

The regeneration study of the spent catalyst was done after recovering the catalyst from the reaction mixture by filtration and washing with acetone followed by activation at 550 °C for 4 and 10 h in air flow. The regenerated catalyst was studied for further reaction cycles under similar reaction conditions. After every reaction cycle, the spent catalyst was recovered and regenerated as described above.

3. Results and discussion

3.1. Catalyst characterization

The powder X-ray diffractograms (Fig. 1) of sulfated zirconia samples at different calcination temperatures exhibited the characteristic peaks of the tetragonal phase at 2θ of 30°, 35°, 50° and 60° indicating the presence of only the tetragonal phase. No phase transformation was observed even after calcination at higher temperature of 800 °C. The crystallinity and the crystallite size of the

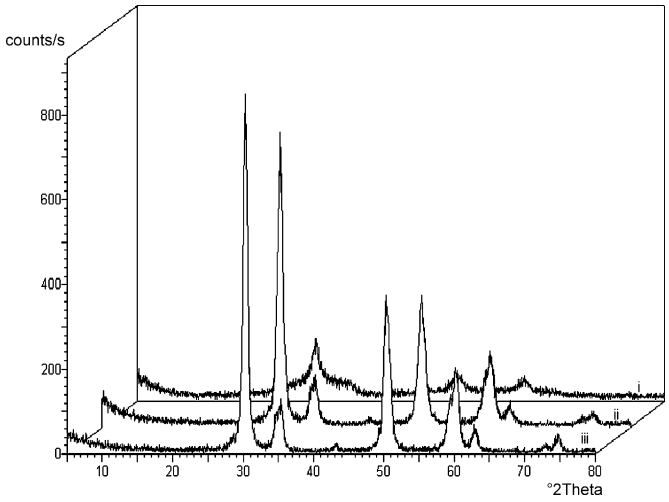

Fig. 1. Powder XRD patterns of sulfated zirconia samples (i) SZ-600, (ii) SZ-700 and (iii) SZ-800.

Table 1
Characterization of sulfated zirconia catalysts.

Catalyst	Crystallite size (nm)	Surface area (m^2/g)	Pore volume (cm^3/g)	Pore diameter (Å)	Sulfur[a] (wt%)	Sulfur[b] (wt%)	Sulfur[c] (wt%)	S/surface area (% S m^{-2})
SZ-600	9	150	0.33	89	3.9	2.9	2.6	0.026
SZ-700	11	96	0.28	120	1.1	1.2	1.1	0.011
SZ-800	14	58	0.25	170	0.6	0.7	0.6	0.010
SZ-reg[d]	9.8	126	0.21	68	1.6	–	–	0.013

[a] Measured by a CHNS/O analyser.
[b] Measured by ICP analysis using HF method.
[c] Measured by ICP analysis using NaOH method.
[d] Regenerated.

samples increased with increasing calcination temperatures from 600 to 800 °C (Table 1). The SZ-600 sample showed less crystallinity, which is attributed to its higher sulfur content (3.9 wt%).

The FT-IR-spectrum (Fig. 2a) of the SZ-600 sample showed the characteristic peaks of inorganic chelating bidentate sulfate at 1238, 1143, 1078, 1041 and 997 cm^{-1}, which are attributed to asymmetric and symmetric stretching frequencies of partially ionized S=O bond and S–O bond [24]. The ionic structure of SO_4^{2-} corresponds to Brönsted acid sites in the sample [24–25]. The SZ-700 and SZ-800 samples showed the decrease in the intensities of these peaks (Fig. 2b and c). In addition, a small peak at 1401 cm^{-1}, which is attributed to the covalent S=O bond [24,25] and corresponds to Lewis acid sites, was observed in the SZ-700 and SZ-800. The presence of this peak with increasing calcination temperatures from 600 to 800 °C showed the transformation of Brönsted acid sites to Lewis acid sites on heating. It also confirmed the reported fact that lower sulfur results in Lewis acid character in sulfated zirconia catalysts [26]. The SZ-800 (Fig. 2c) showed a significant reduction in the peak intensities indicating the significant loss of sulfate species at higher calcination temperature, which is further confirmed by bulk sulfur analysis of the samples.

The bulk sulfur of the samples after calcination at 600 °C was 3.9 wt% as measured by elemental analyzer. The sulfur measured by ICP using HF and NaOH methods was found in the range of 2.6–2.9 wt% (Table 1). The calcination at higher temperatures of 700 and 800 °C resulted in a significant decrease in the sulfur content, which was found in a similar range by both elemental analyzer and ICP. The sulfur content measured by ICP using HF and NaOH methods was also found in a similar range at each calcination temperature, which indicates that all the sulfate species may be present at or near the surface of the samples. This observation is in agreement with the reported fact that during crystallization all bulk sulfur trapped in the pores of the gel network was expelled onto the surface and acted as active surface species [27]. Furthermore, the sulfur per unit surface area was found to be higher in the SZ-600 (0.026), whereas in the SZ-700 and SZ-800 it was in a similar range (0.010–0.011) (Table 1). It showed the presence of significant amount of sulfate species densely distributed on the surface of the SZ-600. The calcination at higher temperatures of 700 and 800 °C resulted in the successive loss of surface sulfate groups; however, uniform concentration of the sulfur content per unit area occurred at both 700 and 800 °C due to the successive decrease in the specific surface area with increasing calcination temperatures.

N_2 adsorption–desorption isotherms (Fig. 3) of the samples showed type IV isotherm, with H3 desorption hysteresis loop. The large increase in the adsorption at higher relative pressure ($p/p_0 > 0.6$) showed the presence of large mesopores. The H3 desorption hysteresis loop indicates the presence of slit shaped pores [23]. The specific surface area and pore volume of the samples decreased from 150 to 58 and 0.33 to 0.25 cm^3/g, respectively due to sintering of the pores with increasing calcination temperatures from 600 to 800 °C, whereas the pore size increased from 89 to 170 Å because of collapsing of the pore walls (Table 1). The successive decrease in the specific surface area was found in the range of 36–39%.

3.2. Surface acidity

3.2.1. NH_3 TPD

Table 2 shows the volume of NH_3 desorbed at different temperatures indicating the total acid sites concentration in the samples. The SZ-600 was found to have 0.339 mmol/g total number of acid sites, whereas the SZ-700 and SZ-800 have 0.446 and 0.436 mmol/g, respectively. On the other hand, acid sites per unit surface area was found to be in increasing order from 0.0023 to 0.0075 with increasing calcination temperatures from 600 to 800 °C. These results were really interesting since the total acidity of sulfated

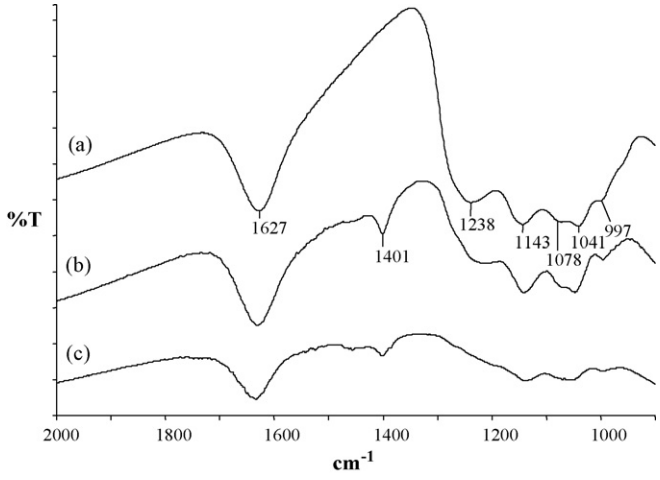

Fig. 2. FT-IR spectra of sulfated zirconia samples (a) SZ-600, (b) SZ-700 and (c) SZ-800.

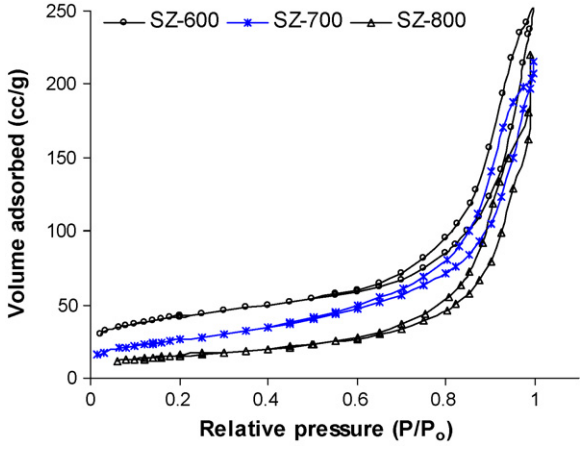

Fig. 3. N_2 adsorption–desorption isotherm of sulfated zirconia samples calcined at different temperatures.

Table 2
Acid sites concentration, cyclohexanol conversion and B/L ratio of sulfated zirconia catalysts.

Catalyst	Temp (°C)	Acid sites (mmol NH_3/g)	Total acid sites (mmol NH_3/g)	Total acid sites/SA (mmol/m^2)	Cyclohexanol conversion (wt%)	py-B band area (A cm^{-1})	py-L band area (A cm^{-1})	B/L ratio
SZ-600	239.7 344.4	0.199 0.140	0.339	0.0023	85	6.35	1.13	5.62
SZ-700	317.8 583.3	0.223 0.223	0.446	0.0046	100	11.66	2.12	4.97
SZ-800	315.0 585.0	0.219 0.217	0.436	0.0075	17	0.437	0.806	0.542
SZO2[a]	298.6 601.8	0.153 0.152	0.305	0.0025	80	5.87	1.61	3.64

[a] Catalyst previously reported [19].

zirconia was expected to decrease with increasing calcination temperatures (>600 °C) due to the significant loss of the sulfate groups.

Furthermore, NH_3 desorption occurred at relatively lower temperature in the SZ-600, indicating the presence of acid sites having weak (~240 °C) and moderate (~344 °C) strengths, whereas the SZ-700 and SZ-800 showed the presence of weak to moderate (315–317 °C) and stronger (583–585 °C) acid sites. The presence of strong acid sites in the SZ-700 and SZ-800, which were completely absent in the SZ-600 clearly showed the formation of these sites after calcination at higher temperatures. This may be explained in terms of the weakly bonded sulfate groups with surface hydroxyl groups in the SZ-600 since there were dense and large population of sulfate groups (as shown by XRD and sulfur analysis) on the surface of the SZ-600. Heating at higher temperatures resulted in the loss of densely populated sulfate groups and a strong bonding of surface sulfate groups with hydroxyl groups occurs providing a strong electron-withdrawing effect of the sulfate groups and thus enhanced the acid strengths of the SZ-700 and SZ-800.

As NH_3 TPD results show the number and strength of total acid sites including both Brönsted and Lewis acid sites, it seems from the above results that there may be a concurrent increase in strong Lewis acid sites at higher calcination temperatures along with a decrease in Brönsted acid sites thus resulting in an overall increase in the amount and strength of acidity. This has been further verified by the measurement of Brönsted acidity from cyclohexanol dehydration reaction and pyridine adsorption to differentiate between Brönsted and Lewis acid sites.

3.2.2. Cyclohexanol dehydration

All three catalysts were found to be active for dehydration of cyclohexanol showing 100% selectivity for cyclohexene, however, with varied conversion values. The SZ-600 sample showed 85% conversion of cyclohexanol indicating the presence of a significant amount of Brönsted acidity, whereas the SZ-700 sample resulted in 100% conversion and the SZ-800 showed the minimum conversion of only 17% (Table 2). It clearly indicated the enhancement of Brönsted acidity with increasing calcination temperature from 600

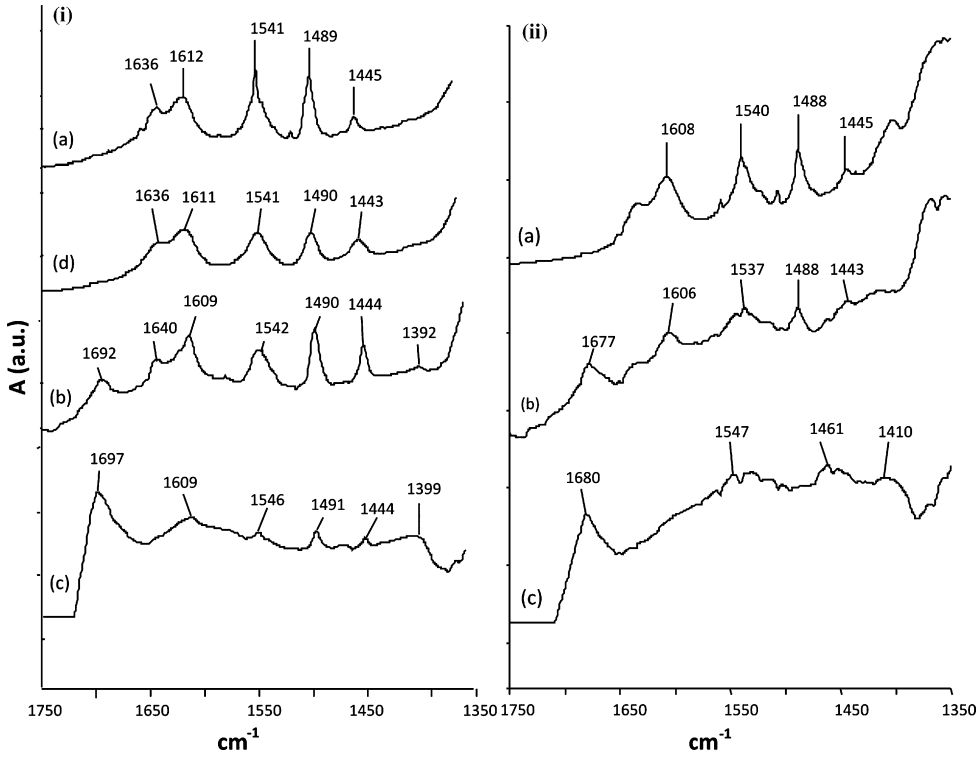

Fig. 4. FT-IR spectra of pyridine adsorbed sulfated zirconia samples (a) SZ-600, (b) SZ-700 and (c) SZ-800 (d) regenerated SZ-600; after pyridine desorption (i) at 150 °C and (ii) at 450 °C.

to 700 °C; however, further increasing the temperature to 800 °C resulted in a drastic decrease in the Brönsted acidity. The activity of the SZ-700 was interesting as it was in contrast to the expected decrease in Brönsted acidity with a concurrent increase in Lewis acidity at higher calcination temperature. It showed that certain degree of dehydroxylation occurring at higher temperature resulted in the enhancement of Brönsted acidity in terms of the strongly bonded sulfate groups with surface hydroxyl groups. Shimizu et al. [28] have also found lower Brönsted acidity and thus less activity of sulfated zirconia calcined at 450 °C for *n*-butane isomerization as compared to the sample calcined at 500 °C due to large population of hydroxyl groups in the sample calcined at 450 °C, which resulted in hydrogen bonds between them and allowed only little interaction with neighboring sulfate groups. It may be noted here that the structural properties of the catalyst such as the amount of sulfate, hydroxyl groups and acidity at a particular calcination temperature may vary because of the variation in synthetic conditions, which strongly influence the properties of the catalyst.

3.2.3. Pyridine adsorption

The FT-IR spectra of pyridine adsorbed catalysts at 150 °C (Fig. 4i) exhibited the IR-bands at 1445, 1489, 1541, 1612 and 1636 cm^{-1}. It indicated the presence of both Brönsted (py-B) and Lewis (py-L) acid sites in all three catalysts as shown by the characteristic bands of py-B and py-L acid sites at 1541 and 1445 cm^{-1}, respectively along with a band at 1489 cm^{-1}, which showed the presence of both py-B and py-L acid sites. Brönsted sites are characterized by the presence of pyridinium ions (NH^+), which are formed by the interaction of pyridine with surface hydroxyl group, whereas co-ordination of the nitrogen lone pair with unsaturated surface cationic centers (Zr^{4+}) acts as a Lewis site. We calculated the area of characteristic bands of 1541 and 1445 cm^{-1} to have an idea of the number of Brönsted and Lewis sites (Table 2). The SZ-700 sample showed the highest and the SZ-800 showed the lowest band area for both the bands. It indicated the highest density of acid sites in the SZ-700, which is in agreement with NH_3 TPD and cyclohexanol conversion values; and the lowest density in the SZ-800, which is in contrast with NH_3 TPD results. However, the B/L ratio (Table 2) was highest for the SZ-600 (5.62) followed by the SZ-700 (4.97); and the SZ-800 showed a very low B/L ratio (0.54).

Besides the above bands, the band corresponding to S=O vibrations at 1401 cm^{-1}, present in the SZ-700 and SZ-800 shifted to a lower frequency at 1392–1399 cm^{-1} after pyridine adsorption (Fig. 4i) as also observed by Song and Kydd [29]. Furthermore, a strong band at 1692–1697 cm^{-1} was observed in the SZ-700 and SZ-800 samples, which was absent in the SZ-600. The intensity of this band remained even after pyridine desorption at higher temperature of 450 °C, when the intensities of other bands were significantly reduced, indicating very high strength of these acid sites (Fig. 4ii). This band (1692–1697 cm^{-1}) may be attributed to a different Lewis acid site resulting from a strongly co-ordinated 'inner' pyridine Lewis complex, which transforms into an adsorbed α-pyridone species as reported for transition alumina [30,31]. In transition aluminas, the strongly co-ordinated 'inner' py-L species (at 1634 cm^{-1}), observed at higher dehydration stages and forming α-pyridone species (Scheme 3), were identified as 'X-sites' and were found to be responsible for high catalytic activity of highly dehydrated aluminas. However, this band is not reported for sulfated zirconia to the best of our knowledge.

In view of the above results obtained from surface acidity measurements done by NH_3 TPD, cyclohexanol dehydration reaction and pyridine adsorption, it has now become clear that all three catalysts have both Brönsted and Lewis acid sites, however, the SZ-700 and SZ-800 have different types of strong Lewis acid sites in addition to normal Brönsted and Lewis acid sites, which may be formed due to a higher degree of dehydroxylation occurring at higher calcination temperatures. Therefore, these samples reflected higher amounts of total acidity as compared to the SZ-600. Though the SZ-800 has very low Brönsted acidity as shown by low conversion value of cyclohexanol dehydration (17%), its total amount and strength of acidity is found in a similar range to the SZ-700 due to the presence of these strong Lewis acid sites. The increasing amount of acid site concentration per unit surface area indicated the formation of higher numbers of these strong Lewis acid sites with increasing calcination temperatures from 600 to 800 °C, which were even compensating the decreasing surface area with increasing calcination temperatures. Furthermore, a certain degree of dehydroxylation occurring at higher temperature (700 °C) resulted in the enhancement of Brönsted acidity in the SZ-700 as shown by highest cyclohexanol conversion (100%).

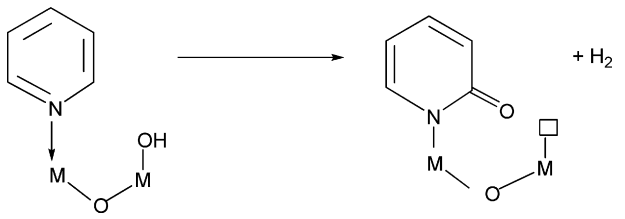

Scheme 3. Formation of adsorbed α-pyridone from strongly co-ordinated pyridine Lewis complex (where, M = Al or Zr and □ shows a co-ordinative vacancy or anion vacancy).

3.3. Catalytic rearrangement of longifolene to isolongifolene and 7-isopropyl-1,1-dimethyltetralin

Table 3 shows the conversion of longifolene to isolongifolene and 7-isopropyl-1,1-dimethyltetralin along with other rearranged products using sulfated zirconia catalysts. All three catalysts showed the conversion of longifolene in a similar range (94–96%) at 180 °C after 1 h. However, the selectivity of the products was found to vary with the catalysts. The catalyst SZ-600 showed 7-isopropyl-1,1-dimethyltetralin (56%) as a major product along with other rearranged products (41%) and a small amount of isolongifolene (3%). The catalyst SZ-700 showed the decrease in the selectivity for 7-isopropyl-1,1-dimethyltetralin and other products to 25% and 38%, respectively, whereas the selectivity for isolongifolene was increased to 37%, which was further increased to 100% for the catalyst SZ-800. No formation of 7-isopropyl-1,1-dimethyltetralin and other products was observed with the catalyst SZ-800.

The sulfated zirconia catalysts prepared after calcination at different temperatures have variation in the structural and textural properties in terms of the crystallinity, crystallite size, sulfur content, surface area, pore volume and pore diameter as observed from Table 1 and Fig. 1. The textural properties may not have a significant effect on the catalytic selectivity since the molecular dimensions of

Table 3
Conversion (wt%) of longifolene and selectivity for rearranged products using sulfated zirconia.

Catalyst	Conversion (wt%)	Selectivity (%)		
		Isolongifolene	7-Isopropyl-1,1-dimethyltetralin	Others[a]
SZ-600	96	3	56	41
SZ-700	95	37	25	38
SZ-800	94	~100	–	–
SZO2[b]	92	~100	–	–

Longifolene = 1.0 g, catalyst = 0.1 g, reaction temperature = 180 °C, time = 1 h.

[a] Tetramethyl hexahydro methano-naphthalene, 7-isopropylidene dimethyl octahydro naphthalene and 7-isopropyl dimethyl octahydro naphthalene rearranged products identified with GC–MS.

[b] Catalyst previously reported [19].

the reactant and product molecules are smaller (~7–10 Å) than the large pores (89–170 Å) of the catalysts and therefore the molecules would diffuse through the pores easily.

The sulfur content and thus the different acid sites present in the catalysts seem to be responsible for the variation in the catalytic selectivity for different rearranged products. The SZ-600 having a lower number of total acid sites (0.339 mmol/g) showed higher selectivity for 7-isopropyl-1,1-dimethyltetralin as compared to the SZ-700 and SZ-800, which have higher numbers of acid sites (0.446 and 0.436 mmol/g, respectively). It showed that total acid sites may not be necessarily catalytic active for a specific reaction and the presence of strong Lewis acidity in the SZ-700 and SZ-800 was not required for the formation of 7-isopropyl-1,1-dimethyltetralin. So, Brönsted acidity may be responsible for the higher selectivity for 7-isopropyl-1,1-dimethyltetralin in the SZ-600. However, the SZ-700 having the highest Brönsted sites (Table 2), which was also confirmed by highest cyclohexanol conversion (100%), showed the decrease in the selectivity for 7-isopropyl-1,1-dimethyltetralin. Thus, Brönsted acidity alone was also not required for the above said selectivity. Then, we compared the selectivity values with the B/L ratio of the samples and the results were found in good agreement. The selectivity for 7-isopropyl-1,1-dimethyltetralin decreased with a decrease in the B/L ratio. The SZ-600 having a higher B/L ratio (5.62) resulted in the higher selectivity, which decreased with a decrease in the B/L ratio (4.97) in the SZ-700. The SZ-800 having a very low B/L ratio (0.54) did not form 7-isopropyl-1,1-dimethyltetralin. It clearly showed that the B/L ratio is very important for the activity of the catalyst rather than the each site. The importance of the optimum B/L ratio has been reported in the literature [32–34]; however, it may vary for the particular reaction as it strongly depends on the synthetic procedure of the catalyst and activation temperature prior to the reaction. For example, Nascimento et al. [32] found the maximum catalytic activity of sulfated zirconia for *n*-butane isomerization when the B/L ratio was about 1, whereas Li and Gonzalez [34] found the optimum ratio of about 0.5 for a similar reaction.

Table 4
Conversion (wt%) of longifolene and selectivity for rearranged products using sulfated zirconia at different reaction time.

Time (min)	Conversion (wt%)	Selectivity (%)		
		7-Isopropyl-1,1-dimethyltetralin	Isolongifolene	Others[a]
1	40	–	~100	–
2	96	–	~100	–
10	96	25	42	33
15	96	41	22	37
30	96	56	8	36
60	96	56	3	41
120	96	56	2	41
240	96	56	2	41

Longifolene = 5 g, catalyst = 0.5 g, reaction temperature = 180 °C.
[a] Tetramethyl hexahydro methano-naphthalene, 7-isopropylidene dimethyl octahydro naphthalene and 7-isopropyl dimethyl octahydro naphthalene rearranged products identified with GC–MS.

The kinetic study carried out using the catalyst SZ-600 showed that the rearrangement of longifolene to isolongifolene was very fast (Table 4). The maximum conversion of longifolene (96%) with ~100% selectivity for isolongifolene was obtained within 2 min of the reaction time, after which the conversion of longifolene remained steady till 4 h. However, the selectivity for isolongifolene

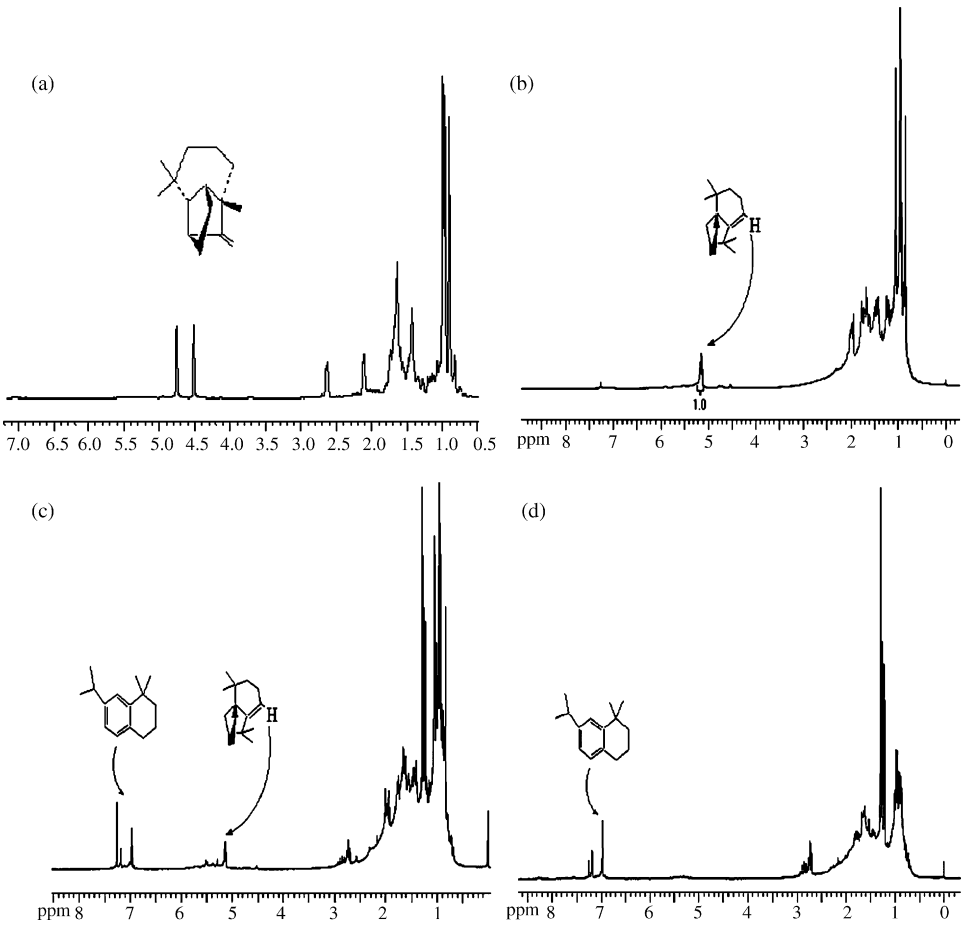

Fig. 5. ^{1}H NMR spectrum of (a) reaction mixture, (b) after 2 min, (c) after 10 min and (d) after 1 h.

significantly decreased and the selectivity for 7-isopropyl-1,1-dimethyltetralin successively increased to 56% along with other products (41%) after 1 h and remained steady till 4 h. A small amount of isolongifolene (2–3%) was found to remain unconverted.

The kinetic study clearly showed that longifolene initially rearranged to isolongifolene which then formed 7-isopropyl-1,1-dimethyltetralin along with other products. It was further confirmed by ^{1}H NMR spectroscopy. The ^{1}H NMR spectrum of the reaction mixture (Fig. 5a) showed two singlets at 4.5 and 4.9 ppm equivalent to two olefinic protons of longifolene. After 2 min of the reaction, the ^{1}H NMR spectrum (Fig. 5b) showed an additional signal at 5.2 ppm (triplet) equivalent to one olefinic proton, indicating the presence of isolongifolene. The absence of the signals in the aromatic region showed no formation of 7-isopropyl-1,1-dimethyltetralin. The ^{1}H NMR spectrum of the reaction mixture after 10 min (Fig. 5c) showed two doublets at 7.1–7.2 ppm (equivalent to two protons) and one singlet at 7.0 ppm (equivalent to one proton) for 7-isopropyl-1,1-dimethyltetralin along with one triplet at 5.2 ppm for isolongifolene. It showed the presence of both isolongifolene and 7-isopropyl-1,1-dimethyltetralin in the reaction mixture after 10 min. The ^{1}H NMR spectrum of reaction mixture after 1 h (Fig. 5d) showed the presence of signals only in the aromatic region for 7-isopropyl-1,1-dimethyltetralin and the absence of the triplet at 5.2 ppm for isolongifolene. It confirmed the formation of 7-isopropyl-1,1-dimethyltetralin by the rearrangement of longifolene via isolongifolene.

The effect of the substrate to catalyst weight ratio was studied with the catalyst SZ-600 by carrying out the reaction at different substrate to catalyst weight ratios ranging from 10 to 100 at 180 °C for 1 h. The substrate to catalyst weight ratio had a significant effect on the selectivity for the products. The data (Table 5) showed that the catalyst gave similar conversions of longifolene in the range of 94–96% with increasing substrate to catalyst weight ratios from 5 to 100, which showed the excellent catalytic activity of sulfated zirconia for the acid catalyzed rearrangement of longifolene. However, the selectivity for the products varied with the substrate to catalyst ratio. The product 7-isopropyl-1,1-dimethyltetralin (52–56%) along with other intermediates (46–41%) was formed only at lower substrate to catalyst weight ratios of 5 and 10. At higher substrate to catalyst weight ratios from 50 to 100, longifolene isomerized selectivity (100%) to isolongifolene. The SZ-700 also showed increased selectivity for 7-isopropyl-1,1-dimethyltetralin from 25 to 29% when used at a lower substrate to catalyst weight ratio of 2 (Table 5) as compared to a higher substrate to catalyst weight ratio of 10 (Table 3).

The above results showed that a small number of acid sites were sufficient to catalyze longifolene to isolongifolene even at a higher substrate to catalyst ratio of 100. However, these acid sites were insufficient for further rearrangement of isolongifolene to 7-isopropyl-1,1-dimethyltetralin. It could be explained in terms of the lower availability of acid sites as compared to longifolene, which may be covered with longifolene and therefore the probability of isolongifolene to interact with acid sites to be further converted into 7-isopropyl-1,1-dimethyltetralin is less. However, with increase in the amount of the catalyst, higher numbers of acid sites were available and thus isolongifolene molecules could contact the sites resulting in further rearrangement. It showed the requirement of a higher number of acid sites for the formation of 7-isopropyl-1,1-dimethyltetralin and not necessarily the strength of the catalyst. As shown by NH_3 TPD data, the catalyst SZ-600 has weak (240 °C) to moderate (344 °C) Brönsted acid sites, and therefore, we assume that a higher number of weak to moderate Brönsted acid sites are required for the formation of 7-isopropyl-1,1-dimethyltetralin. In our previous report [19] we have found that isomerization of longifolene to isolongifolene is a Brönsted acid catalyzed reaction. The present study shows that further rearrangement of isolongifolene to 7-isopropyl-1,1-dimethyltetralin requires a higher number of weak to moderate Brönsted acid sites along with a optimum B/L ratio, which is found in the range of 3.6–5.6 under the experimental conditions studied.

The sulfated zirconia catalyst (SZO2) previously reported to give isolongifolene selectively at a substrate to catalyst weight ratio of 10 [19] was also studied at lower substrate to catalyst weight ratios of 2 and 5 and was found to form 7-isopropyl-1,1-dimethyltetralin (38%) at a substrate to catalyst ratio of 2 (Table 5). This also confirmed the requirement of a higher number of acidic sites for the formation of 7-isopropyl-1,1-dimethyltetralin. This sample was found to have weak (~298 °C) along with strong (~601 °C) acid sites with a total acid sites concentration of 0.305 mmol NH_3/g (Table 2). The B/L ratio of this catalyst after pyridine adsorption was found to be 3.64 (Table 2). It further confirmed the requirement of a certain B/L ratio for the above said formation.

3.4. Catalyst regeneration

Thermally regenerated catalyst (SZ-600) showed a similar conversion of longifolene (94%) till the third reaction cycles; however, the selectivity for 7-isopropyl-1,1-dimethyltetralin significantly decreased only after the first cycle, i.e., from 56 to 10% and the selectivity for isolongifolene was increased to 46% while other products were obtained in a similar amount (44%) (Table 6). In the next cycle, the regenerated catalyst showed a further decrease in the selectivity for 7-isopropyl-1,1-dimethyltetralin (5%) and others (37%) and an increase in the selectivity for isolongifolene to 58%, which was found to be similar after the third cycle.

The decrease in the selectivity for 7-isopropyl-1,1-dimethyltetralin with a regenerated catalyst may be due to the deactivation of some of the Brönsted acid sites responsible

Table 5
Conversion (wt%) of longifolene and selectivity for rearranged products using sulfated zirconia at different substrate to catalyst ratio.

Catalyst	Substrate/catalyst ratio	Conversion (wt%)	Selectivity (%)		
			7-Isopropyl-1,1-dimethyltetralin	Isolongifolene	Others[a]
SZ-600	5	96	52	2	46
SZ-600	10	96	56	3	41
SZ-600	50	95	–	~100	–
SZ-600	70	95	–	~100	–
SZ-600	100	94	–	~100	–
SZ-700	2	94	29	6	65
SZO2[b]	2	94	38	9	63
SZO2	5	94	~100	-	–

Reaction temperature = 180 °C, time = 1 h.

[a] Tetramethy hexahydro methano-naphthalene, 7-isopropylidene dimethyl octahydro naphthalene and 7-isopropyl dimethyl octahydro naphthalene rearranged products identified with GC–MS.

[b] Catalyst previously reported [19].

Table 6
Conversion (%) of longifolene and selectivity for rearranged products using regenerated sulfated zirconia catalyst.

Reaction cycle	Conversion (wt%)	Selectivity (%)		
		Isolongifolene	7-Isopropyl-1,1-dimethyltetralin	Others[a]
Fresh catalyst	96	3	56	41
I	94	46	10	44
II	94	58	5	37
III	94	58	5	37

Substrate/catalyst weight ratio = 10, reaction temperature = 180 °C, time = 1 h.

[a] Tetramethy hexahydro methano-naphthalene, 7-isopropylidene dimethyl octahydro naphthalene and 7-isopropyl dimethyl octahydro naphthalene rearranged products identified with GC–MS.

for its formation which could not be regenerated completely by simple thermal heating at 550 °C for 4 h or even for 10 h in air flow. Thus less availability of higher numbers of Brönsted acid sites decreased the tetralin selectivity. However, the successive increase in the selectivity for isolongifolene showed that a small number of acid sites needed for the formation of isolongifolene could be easily regenerated. The possible reasons for the deactivation of these sites may be (i) change in structural and textural properties and transformation of the active tetragonal phase into the inactive monoclinic phase, (ii) coke deposition on the active sites, and (iii) change in surface acidity.

This was confirmed by the characterization of a regenerated catalyst. The surface area, pore volume and pore diameter was found to decrease along with a carbon content 0.08 wt% higher as compared to the fresh catalyst, which indicates the blockage of the pores by the deposition of coke. The crystallinity of this catalyst was slightly higher than the fresh one, however, having the tetragonal crystalline phase (crystallite size 9.8 nm). The bulk sulfur was found to be lower (1.6 wt%) indicating the loss of sulfur during the reaction. The FT-IR spectrum of the used catalyst showed the peaks of adsorbed species of substrate and/or products (in the region of ~1400–1600 cm^{-1}) on the surface of the catalyst (Fig. 6i). The regenerated catalyst (550 °C, 4 h in air flow) (Fig. 6 ii) did not show the peaks of adsorbed species; however, a peak at 1401 cm^{-1} was present, which may be due to (i) S=O vibrations (if there happened any qualitative variation in the acid sites during the reaction as this peak was absent in the fresh SZ-600) or (ii) coke deposition. The possibility of (i) has been ruled out because after pyridine adsorption this peak should be shifted to lower wave number as was found in the SZ-700 and SZ-800 samples; however, it was not the case

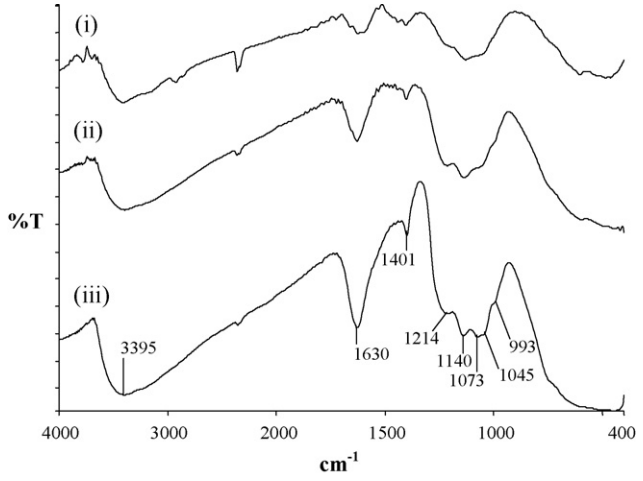

Fig. 6. FT-IR spectra of: (i) used SZ-600; regenerated (ii) at 550 °C, 4 h in air flow and (iii) at 550 °C, 10 h in air flow.

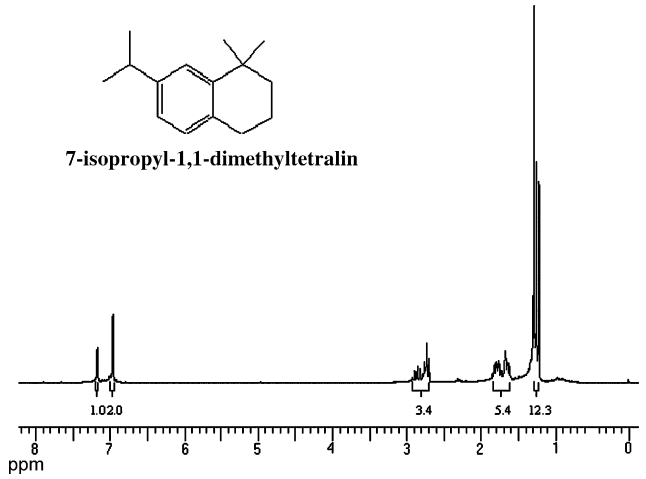

Fig. 7. ^{1}H NMR spectrum of 7-isopropyl-1,1-dimethyltetralin.

(Fig. 4i-d). Therefore, the presence of this peak indicated the coke deposition on some of the active acid sites, which remained present even after heating for longer time of 10 h in a flow of air (Fig. 6iii). The pyridine adsorption on this regenerated catalyst showed the presence of Brönsted and Lewis acid sites similar to the fresh one (Fig. 4i-d); however, the calculated B/L ratio was lower, i.e., 2.66 as compared to the fresh catalyst having a B/L ratio of 5.62.

Based on the above results the decrease in the catalytic selectivity for 7-isopropyl-1,1-dimethyltetralin in regenerated catalysts may be attributed to a decrease in the B/L ratio, which is dependent on the sulfur content of the catalyst. The loss of sulfur during the reaction may occurred due to the formation of an organo-sulfur complex on the active sites on the surface as well as within the pores of the catalyst. Though heating in air flow has regenerated few active sites and increased the selectivity for isolongifolene, but not all sites necessary for higher selectivity for 7-isopropyl-1,1-dimethyltetralin. A small amount of coke deposition, e.g., only 0.06 wt% may result in complete deactivation of sulfated zirconia for *n*-butane isomerization [34]. The loss in sulfur content resulted in a change in surface acidity in terms of the acid sites ratio and thus in the catalyst selectivity for 7-isopropyl-1,1-dimethyltetralin. It clearly showed the role of the optimum B/L ratio in the selective formation of 7-isopropyl-1,1-dimethyltetralin under the experimental conditions studied.

3.5. Characterization of the products

The major product, 7-isopropyl-1,1-dimethyltetralin, was separated from the reaction mixture and purified by silica gel column (60–120 mesh) with petroleum ether. It was characterized by ^{1}H NMR spectroscopy (Fig. 7) and GC–MS analysis (Fig. 8i).

^{1}H NMR ($CDCl_3$): δ 7.10–7.20 (d, 2H, ArH), 7.0 (s, 1H, ArH), 2.60–2.90 (3H), 1.50–1.90 (4H), 1.20–1.40 (12H). The *m*/*z* for molecular ion $[M]^+$ of 7-isopropyl 1,1-dimethyltetralin ($C_{15}H_{22}$) is 202.

The other major rearranged intermediates such as tetramethylhexahydromethanonaphthalene [M^+ 204] (Fig. 8ii) and 7-isopropylidenedimethyloctahydronaphthalene [M^+ 204] (Fig. 8iii) and an octalin derivative, i.e., 7-isopropyldimethyloctahydronaphthalene [M^+ 206] (Fig. 8iv) was also identified by analyzing the reaction mixture by GC–MS (Fig. 8).

4. Mechanistic pathway of rearrangement of longifolene to isolongifolene and 7-isopropyl-1,1-dimethyltetralin

Dev [35] has elegantly explained the longifolene chemistry and formation of isolongifolene via several possible schemes.

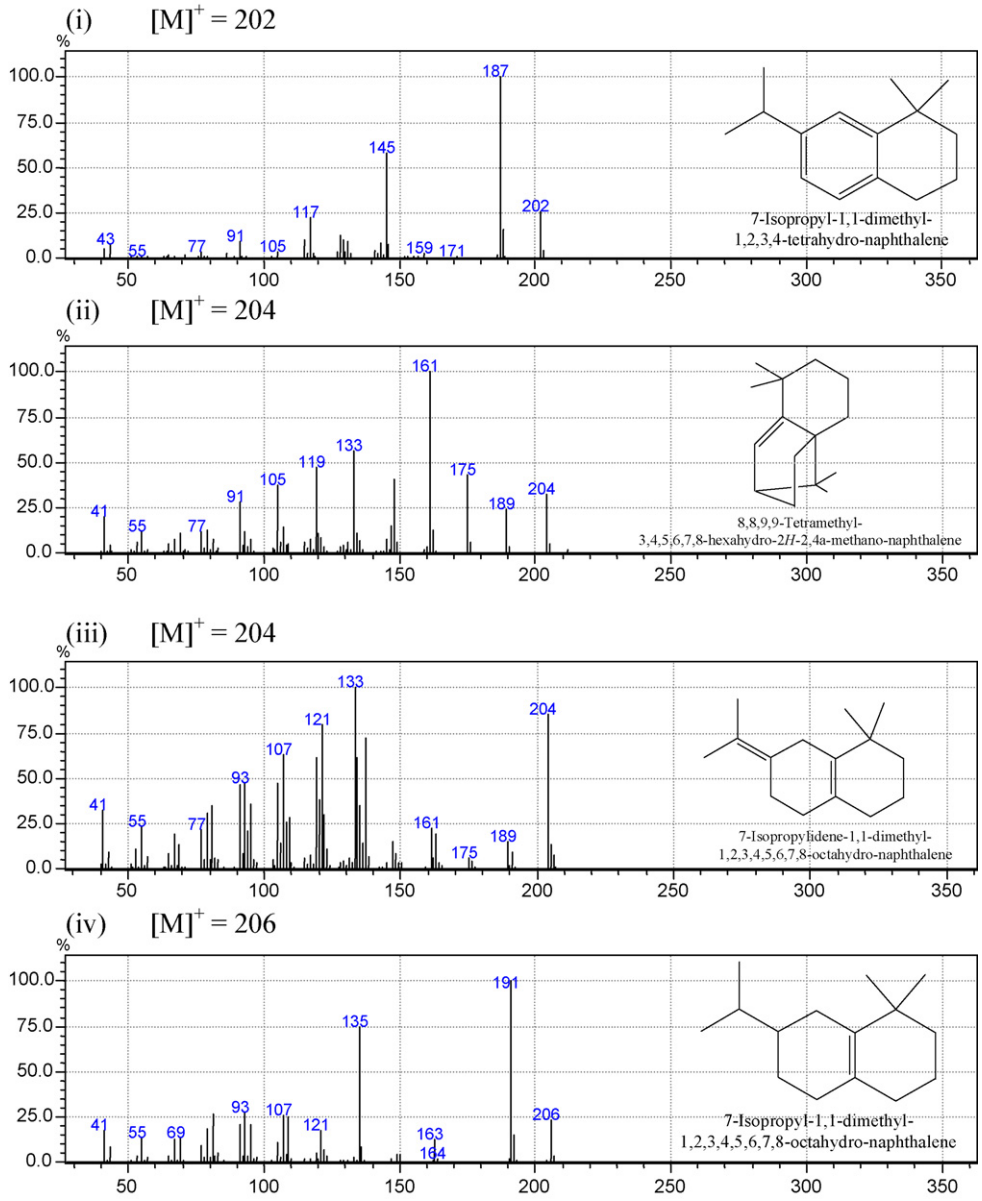

Fig. 8. GC-mass spectra of (i) 7-isopropyl-1,1-dimethyltetralin (7-isopropyl-1,1-dimethyl-1, 2,3,4-tetrahydro-naphthalene), (ii) isomerized, (iii) intermediate isomerized and (iv) rearranged octalin derivative product.

We have tried to summarize the formation of 7-isopropyl-1,1-dimethyltetralin via isolongifolene in Scheme 4. Longifolene (I) is a strained high energy molecule having an exo-olefinic double bond, which has strong affinity towards the protons (available from the acid catalyst) to form carbonium ion (a). The carbonium ion thus formed is highly reactive and undergoes a series of 1, 2 shifts of $-CH_3$ group, hydrogen and C–C σ bonds to form (b), which then rearranges to a comparatively lower energy configuration forming isolongifolene (II). However, isolongifolene is still a high energy molecule by virtue of the presence of the strained bicyclo [2.2.1] heptane system and an olefinic double bond inside the ring, and therefore, in the presence of highly acidic conditions, it takes proton and again forms carbonium ion (b), which undergoes several elimination/rearrangement/disproportionation to attain a stable molecular system such as 7-isopropyl-1,1-dimethyltetralin (III).

Our theoretical calculations (Table 7) for free energy and entropy for the stable structures drawn (Fig. 9) for longifolene (I), isolongifolene (II) and 7-isopropyl-1,1-dimethyltetralin (III) confirmed these successive rearrangements. Lower free energy and higher entropy values for II and III favor their formations.

The formation of tetralin (III) and also octalin (IV) derivatives may be explained in terms of sterically crowded structures of longifolene (I) and isolongifolene (II), which can divert the normal reaction pathways resulting in sterically diverted products through other pathways such as elimination/rearrangement/disproportionation [35]. The intermediate carbonium ion (b) is a key intermediate for the formation of these aromatic hydrocarbons through the bicyclic cation (d).

Table 7
Theoretical calculations for free energy and entropy at 25 °C.

Compound	Free energy (G) (kcal/mol)	Entropy (S) (kcal/mol K)
Longifolene	192.657	125.166
Isolongifolene	191.821	128.818
7-Isopropyl-1,1dimethyltetralin	176.313	133.459

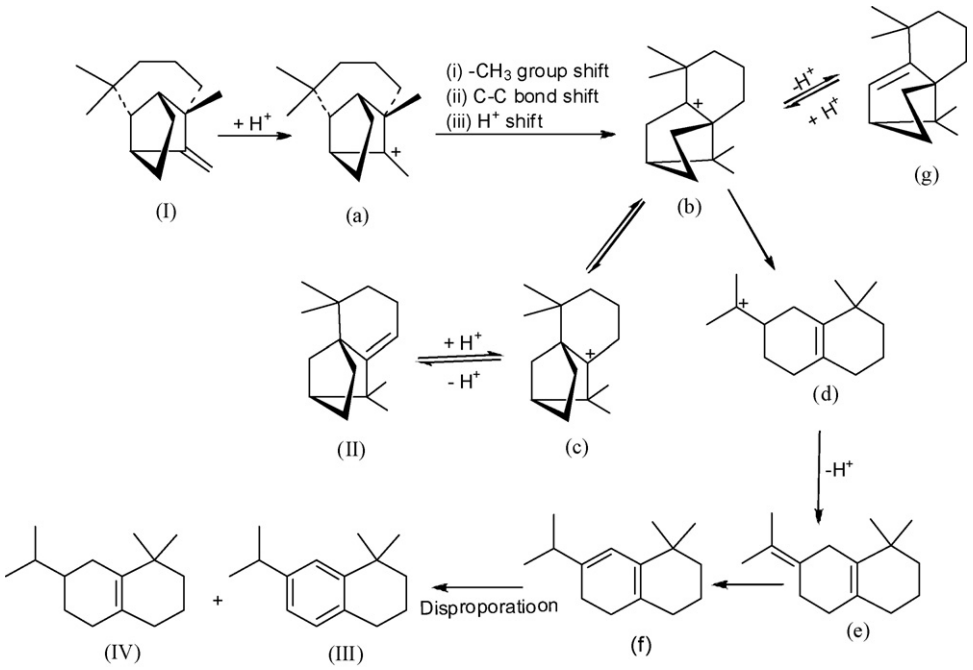

Scheme 4. Mechanistic pathways of rearrangement of longifolene to isolongifolene and 7-isopropyl-1,1-dimethyltetralin.

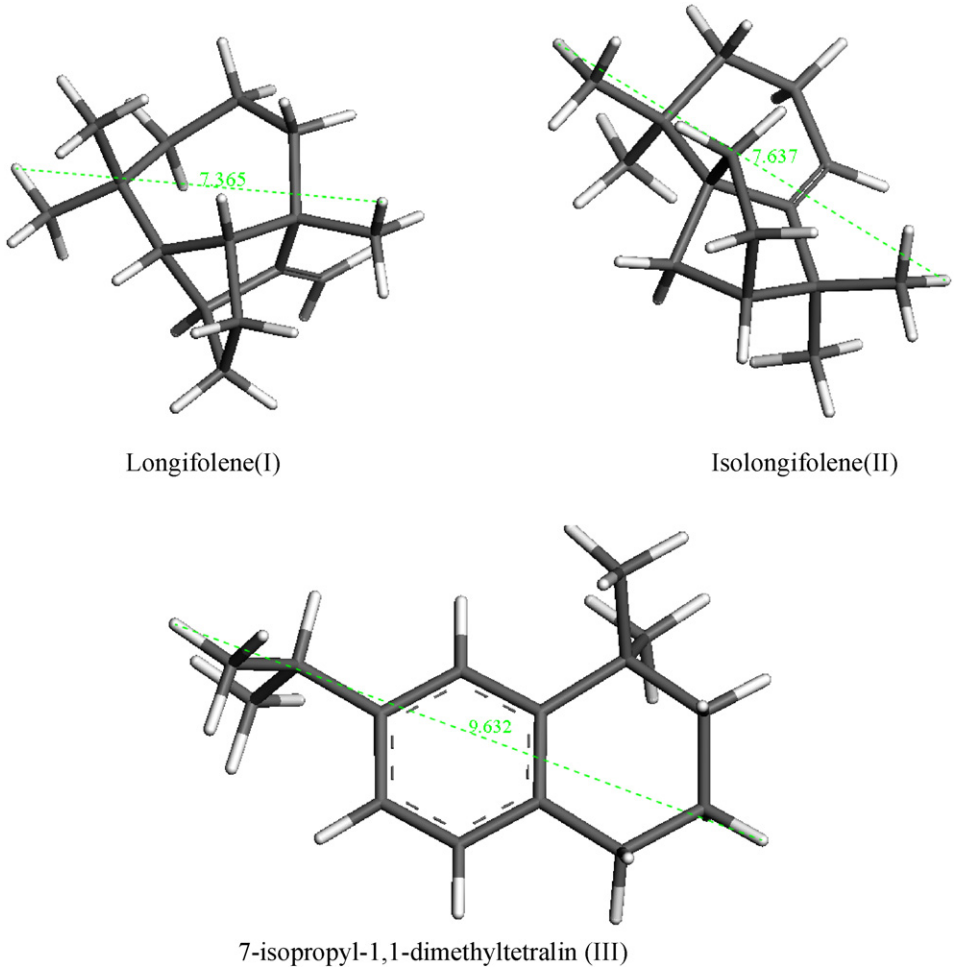

Fig. 9. Theoretical stable structures of longifolene (I) isolongifolene (II) and 7-isopropyl-1,1-dimethyltetralin (III) drawn by Materials Studio.

By comparing the data shown in Table 5 with Scheme 4 and acidity measurement of the catalysts, we suggest that at the substrate to catalyst weight ratios of 50–100, i.e., in the presence of a less number of weak to moderate Brönsted acid sites, intermediate carbonium ion (b) is formed, which rearranges to isolongifolene via carbonium ion (c). However, at substrate to catalyst weight ratios of 5 and 10, i.e., in the presence of a higher number of Brönsted acid sites available, isolongifolene further takes proton and forms (c), which rearranges to (d) via (b) to form tetralin (III) and octalin (IV) derivatives through rearrangement/elimination/disproportionation.

The GC-mass spectra (Fig. 8) of the reaction mixture showed the presence of tetramethylhexahydromethanonaphthalene (ii), 7-isopropylidenedimethyloctahydro naphthalene (iii) and 7-isopropyldimethyloctahydronaphthalene (iv), which are the rearranged products, i.e., (g), (e) and IV, respectively as shown in Scheme 4. It showed the possibility of the reaction occurring via the pathways as shown in Scheme 4.

5. Conclusions

Nano-crystalline sulfated zirconia catalysts have been found to show excellent catalytic activity for the rearrangement of longifolene under the solvent free conditions. However, the selectivity for the rearranged products namely isolongifolene and 7-isopropyl-1,1-dimethyltetralin was strongly influenced by the surface acidity in terms of an optimum B/L ratio as well as by the amount of the catalyst. For example, ~100% isolongifolene can be obtained using a less amount of the catalyst, whereas for 7-isopropyl-1,1-dimethyltetralin a higher amount of catalyst is required. Kinetic and ^{1}H NMR spectroscopic studies confirm the formation of 7-isopropyl-1,1-dimethyltetralin through further rearrangement of isolongifolene. Acidity measurements by NH_3 TPD and pyridine adsorption confirm that presence of a higher number of total acid sites and strong Lewis acid sites are not necessarily catalytic active for the present rearrangement reaction under the experimental conditions studied. On the other hand, a higher number of weak to moderate Brönsted acid sites with an optimum B/L ratio in the range of 3.6–5.6 are required for the formation of 7-isopropyl-1,1-dimethyltetralin. The catalyst having a higher B/L ratio (5.6) showed higher selectivity (56%) for 7-isopropyl-1,1-dimethyltetralin.

The regenerated catalyst was found to have similar conversions of longifolene as that of fresh one, however, with increased selectivity for isolongifolene and decreased selectivity for 7-isopropyl-1,1-dimethyltetralin, which may be attributed to the loss of sulfur during the reaction by forming an organo-sulfur complex deposited as coke on the active sites of the catalyst. The decrease in the sulfur content resulted in the decrease in the B/L ratio, thus significantly decreasing the catalyst selectivity for 7-isopropyl-1,1-dimethyltetralin.

Acknowledgments

Authors are thankful to CSIR Network Programme on Catalysis. Authors are also thankful to Mr. Renjith Pillai for theoretical calculations; and to Analytical Science Discipline for providing instrumental analysis namely to Dr. (Mrs.) P.A. Bhatt for X-ray, Mr. Vinod Agarwal for FT-IR, Mr. Viral for elemental sulfur and Mr. Prashant K.P. for surface area analysis.

References

[1] M. Hino, S. Kobayashi, K. Arata, J. Am. Chem. Soc. 101 (1979) 6439.
[2] T. Yamaguchi, Appl. Catal. A: Gen. 61 (1990) 1.
[3] A. Sayari, Y. Yang, X. Song, J. Catal. 167 (1997) 346.
[4] X. Li, K. Nagaoka, R. Olindo, J.A. Lercher, J. Catal. 238 (2006) 39.
[5] J.M. Grau, J.M. Parera, Appl. Catal. A: Gen. 162 (1997) 17.
[6] D. Farcasiu, J.Q. Li, S. Cameron, Appl. Catal. A: Gen. 154 (1997) 173.
[7] Y.-W. Suh, J.-W. Lee, H.-K. Rhee, Appl. Catal. A: Gen. 274 (2004) 159.
[8] X. Song, A. Sayari, Catal. Rev. Sci. Eng. 38 (3) (1996) 329.
[9] G.D. Yadav, J.J. Nair, Micropor. Mesopor. Mater. 33 (1999) 1.
[10] K. Tanabe, H. Hattori, T. Yamaguchi, Crit. Rev. Surf. Chem. 1 (1990) 1.
[11] (a) G.D. Yadav, J.J. Nair, J. Chem. Soc. Chem. Commun. (1998) 2369; (b) G.D. Yadav, J.J. Nair, Langmuir 16 (2000) 4072.
[12] L. Grzona, N. Comelli, O. Masini, E. Ponzi, M. Ponzi, React. Kinet. Catal. Lett. 69 (2000) 271.
[13] http://www.thegoodscentscompany.com/data/rw10200031.html.
[14] H.H. Zeiss, M. Arakawa, J. Am. Chem. Soc. 76 (1954) 1653.
[15] R.E. Beyler, G. Ourisson, J. Org. Chem. 30 (1965 2838).
[16] R.R. Sobti, S. Dev, Tetrahedron 26 (1970) 649.
[17] C. Sell, in: D.H. Pybus, C.S. Sell (Eds.), The Chemistry of Fragrances, Royal Society of Chemistry, Cambridge, 1999, p. 81.
[18] (a) S.C. Bisarya, U.R. Nayak, S. Dev, Tetrahedron Lett. (1969) 2323; (b) S.C. Bisarya, U.R. Nayak, S. Dev, B.S. Pandey, J.S. Yadav, H.P.S. Chawla, J. Indian Chem. Soc. 55 (1978) 1138.
[19] B. Tyagi, M.K. Mishra, R.V. Jasra, Catal. Commun. 7 (2006) 52.
[20] B. Tyagi, M.K. Mishra, R.V. Jasra, J. Mol. Catal. 276 (2007) 47–56.
[21] B.D. Cullity, S.R. Stock, Elements of X-ray Diffraction, 3rd ed., Prentice Hall, Upper Saddle River, NJ, 2001, p. 388.
[22] C. Sarzanini, G. Sacchero, F. Pinna, M. Signoretto, G. Cerrato, C. Morterra, J. Mater. Chem. 5 (1995) 353.
[23] S.J. Gregg, K.S.W. Sing, Adsorption, Surface Area and Porosity, 2nd ed., Academic Press, New York, 1982.
[24] T. Yamaguchi, T. Jin, K. Tanabe, J. Phys. Chem. 90 (1986) 3148.
[25] M. Bensitel, O. Saur, J.C. Lavalley, B.A. Morrow, Mater. Chem. Phys. 19 (1988) 147.
[26] Manish. K. Mishra, B. Tyagi, R.V. Jasra, Ind. Eng. Chem. Res. 42 (2003) 5727.
[27] D. Ward, E.I. Ko, J. Catal. 150 (1994) 18.
[28] K. Shimizu, N. Kounami, H. Wada, T. Shishido, H. Hattori, Catal. Lett. 54 (1998) 153.
[29] S.X. Song, R.A. Kydd, J. Chem. Soc., Faraday Trans. 94 (1998) 1333.
[30] H. Knözinger, Adv. Catal. 25 (1976) 184.
[31] C. Moreterra, G. Magnacca, Catal. Today 27 (1996) 497, and ref. within.
[32] A. Nascimento, C. Akratopoulou, M. Oszagyan, G. Coudurier, C. Travers, J.F. Joly, J.C. Vedrine, Proceedings of 10th International Congress on Catalysis, Budapast, Hungary, July, 1992, p. 1185.
[33] C. Morterra, G. Cerrato, V. Bolis, S. Di Ciero, M. Signoretto, J. Chem. Soc. Faraday Trans. 93 (1997) 1179.
[34] B. Li, R.D. Gonzalez, Catal. Today 46 (1998) 55.
[35] S. Dev, Acc. Chem. Res. 14 (1981) 82.